Low-temperature Synthesis of Graphene-CdLa$_2$S$_4$ Nanocomposite as Efficient Visible-light-active Photocatalysts

Lei Zhu and Won-Chun Oh[†]

Department of Advanced Materials Science & Engineering, Hanseo University, Seosan 356-706, Korea

(Received March 15, 2015; Accepted May 7, 2015)

ABSTRACT

We report the facile synthesis of graphene-CdLa$_2$S$_4$ composite through a facile solvothermal method at low temperature. The as-prepared products were characterized by X-ray diffraction (XRD) and by Scanning electron microscopy (SEM) with energy dispersive X-ray (EDX) analysis and BET analysis, revealing the uniform covering of the graphene nanosheet with CdLa$_2$S$_4$ nanocrystals. The as-prepared samples show a higher efficiency for the photocatalytic degradation of typical MB dye compared with P25 and CdLa$_2$S$_4$ bulk nanoparticles. The enhancement of visible-light-responsive photocatalytic properties by decolorization of Rh.B dye may be attributed to the following causes. Firstly, graphene nanosheet is capable of accepting, transporting and storing electrons, and thus retarding or hindering the recombination of the electrons with the holes remaining on the excited CdLa$_2$S$_4$ nanoparticles. Secondly, graphene nanosheet can increase the adsorption of pollutants. The final cause is that their extended light absorption range. This work not only offers a simple way to synthesize graphene-based composites via a one-step process at low temperature but also a path to obtain efficient functional materials for environmental purification and other applications.

Key words : Low temperature synthesis, Visible Light, Photocatalytic, Graphene, CdLa$_2$S$_4$

1. Introduction

Graphene, a semi-metal material with zero band gap, has attracted intense attention since it was discovered by Geim *et al.* in 2004.[1] The novel two-dimensional material possesses excellent electrical and optical properties, large specific surface area, and outstanding mechanical properties.[2,3] Recently, Peak *et al.* proved that graphene nanosheets can act as electronic conductive channels to improve the electrochemical performance of the graphene–SnO$_2$ composite.[4] Seger and Kamat demonstrated that graphene is an effective support material to disperse Pt nanoparticles.[5] Therefore, graphene is expected to serve as a scaffold to anchor nanoscale semiconductor photocatalyst and as a photosensitizer to enhance their photocatalytic activity under visible-light illumination at the same time.

Semiconduction photocatalysts are widely used in the destruction of organic pollutants. Now TiO$_2$ is the focus. However, its photo efficiency and photoresponse are insufficient due to the high rate of recombination of electrons and holes.[6] In addition, due to its large bandgap energy of 3.0 -3.2 eV, it can only be activated by UV light, which accounts only 3 - 4% of the sunlight spectrum.[7] Therefore, this makes it necessary to design new photocatalysts to meet the requirements of future applications. Metal sulfides, as important semicon-

ductors, have been used in many new application areas, such as quantum size effect, non-linear optical properties, laser communication and light-emitting diodes,[8] hydrogenation processes, and CO-shift reactions.[9,10] Also of broad interest are the photocatalytic properties of metal sulphides.[11]

The graphene-metal sulfide composites were traditionally prepared using graphene oxide (GO) as a starting material, and the oxygen-containing groups in GO controlled the decoration of nanoparticles without aggregation. In addition, the reduction of GO led to graphene-based composites with good charge transport property. Graphene-CdS composites were studied previously,[12,13] and the fluorescence quenching effect of the composites indicated the effective transfer of photo-excited electrons from CdS to graphene and suppressed the recombination of photo-generated electron-hole pairs, thereby enhancing visible-light-induced photodegradation activity. Huating *et al.* reported a rapid microwave-assisted method for synthesizing graphene nanosheets-zinc sulfide nanocomposites and their application in photocatalysis.[14] The as-prepared graphene-based nanocomposites show an excellent photocatalytic activity toward the photodegradation of methylene blue. The detailed formation and photocatalytic mechanism were also provided in that report.

As a ternary semiconductor chalcogenide, CdLa$_2$S$_4$ has a strong absorption in the visible light region with band gap energy of 2.1 ev; therefore, it has become a good catalyst for the photo-degradation of organic pollutants and photoproduction of hydrogen from water over the past few years.[15,16] Kale *et al.* first reported the photocatalytic activity of CdLa$_2$S$_4$ with Pt loading for H$_2$ production in water/

[†]Corresponding author : Won-Chun Oh
 E-mail : wc_oh@hanseo.ac.kr
 Tel : +82-41-660-1337   Fax : +82-41-688-3352

methanol solution[15]. Hou *et al.* found that the coupling of CdS nanoparticles with $CdLa_2S_4$ microspheres led to a significant increase in the photocatalytic H_2 production rate; nevertheless, Pt-loading was still required for H_2 evolution.[17] However, to date, very few studies in the literature have reported on the synthesis the $CdLa_2S_4$ based on graphene nanosheets and applications on photo-degradation of organic pollutants.
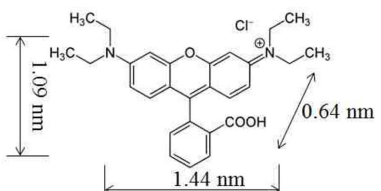
In this paper, we report the synthesis of graphene nanosheets coated with $CdLa_2S_4$ nanoparticles directly via a facile solvothermal method. The intrinsic characteristics of resulting composite were studied by X-ray diffraction (XRD) and Scanning electron microscopy (SEM) with energy dispersive X-ray (EDX) analysis. The photocatalytic activity of the as-synthesized graphene-$CdLa_2S_4$ composite was evaluated by degradation of different organic dyes methylene blue (MB) and rhodamine B (Rh.B) in aqueous solution under visible light irradiation ($\lambda > 400$ nm).

2. Experimental Procedure

2.1 Materials

Ethylene glycol and anhydrous ethanol were purchased from Daejung Chemical Co. Ltd., Korea. Sulfuric acid (H_2SO_4), potassium permanganate ($KMnO_4$), hydrogen peroxide (H_2O_2), $(CH_3COO)_2Cd.2H_2O$, $La(NO_3)_3.H_2O$ and $Na_2S_2O_3$ were supplied by Daejung Chemical Co. Ltd., Korea. The MB ($C_{16}H_{18}N_3S \cdot Cl$, 99.99+%) and Rh.B ($C_{28}H_{31.}ClN_2O_3$, 99.99+%) were used as model pollutant, and were purchased from Duksan Pure Chemical Co., Ltd, Korea. Table 1 shows the structure and properties of MB and Rh.B. Ammonium hydroxide (NH_3H_2O) was purchased from Duksan Pure Chemical Co. Ltd., Korea and used as received. Titanium oxide nanopowder (TiO_2, < 25 nm, 99.7%) with anatase structure was used as control sample and was purchased from Sigma-Aldrich Chemistry, USA. All chemicals were used without further purification, and all experiments were carried out using distilled water.

2.2 Synthesis of graphene oxide (GO)

In brief, 10 g of natural graphite powders were mixed with conc. H_2SO_4 (230 ml) at 0°C with vigorous magnetic stirring. In the next step, 30 g of $KMnO_4$ were slowly added to the flask, and the temperature was kept below 15°C. The resulting mixture was stirred at 35°C until it became pasty brownish, and it was then diluted to 150 ml using de-ionized (DI) water with continued stirring at below 90°C. After adding water, the container was sealed and kept at 100°C with vigorous stirring for 30 min, followed by the addition of 20% H_2O_2, drop by drop, within 5 min. The mixture was then washed several times with water, acetone, and 10% HCl solution to eliminate residual metal ions. The mixture was then heat treated in a dry oven at 90°C for 12 h to obtain graphite oxide powder. For the preparation of graphene oxide, 200 mg of graphite oxide powder were mixed in 200 ml DI water (1 mg/ml), stirred for 30 min, and ultrasonicated for 1 h. The resulting solutions were filtered and washed several times with hot water and kept in a dry oven for 6 h to achieve graphene oxide powder. In order to obtain graphene as a control sample, graphene oxide was reduced via a mild chemical method according to our previous research.[18]

2.3 Synthesis of graphene-CdLa₂S₄ (GR-CdLa₂S₄) nanocomposites

In a typical experiment, about 200 mg GO was dispersed in 80 ml ethylene glycol and then exfoliated to generate graphene oxide nanosheet (GONS) dispersion solution by ultrasonication for 1 h. Subsequently, 0.386 mM $(CH_3COO)_2Cd.2H_2O$ and 0.772 mM $La(NO_3)_3.H_2O$ were added to the GONS aqueous dispersion, followed by ultrasonication for 20 min. Afterwards, sodium thiosulfate anhydrous ($Na_2S_2O_3$) and 10 mL ammonium hydroxide (NH_3H_2O) were added to the mixture under vigorous stirring at 120°C for another 12 h. The ammonia ensured maximal charge so as to prevent the aggregation of graphene oxide caused by the salt effect,[19] which was in favor of the uniform distribution of $CdLa_2S_4$ on GNS. The final product was rinsed with distilled water and ethanol for several times and dried at 60°C for 12 h. Pure $CdLa_2S_4$ nanoparticles were also synthesized by the same procedure except that no GONS was used. The preparation conditions and a schematic illustration are shown in Fig. 1 and Fig. 2(a), respectively.

2.4 Characterization

Crystallographic structure of the composites photocatalysts were obtained by XRD (Shimatz XD-D1, Japan) at room temperature with CuKα radiation ($\lambda = 0.154056$ nm) and a graphite monochromator, operated at 40 KV and 30 mA. The morphologies of the photocatalysts were analyzed by SEM (JSM-5200 JOEL, Japan) at 3.0 keV, which was equipped with an energy dispersive X-ray analysis system (EDX). The BET surface areas of the nanocomposite photocatalysts were determined through nitrogen adsorption at 77 K using a BET analyzer (Monosorb, USA). All the samples were degassed at 623 K before the measurement. The
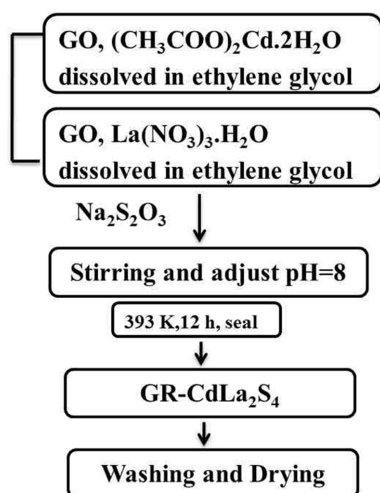
Table 1. The Molecular Structure and Absorbance Maximum (λ_{max}) of Organic Dyes

Organic dyes	Molecular structure	λ_{max}
Methylene blue (MB)		665 nm
Rhodamine B (Rh.B)		554 nm

Fig. 1. Flow chart about synthesize GR-CdLa$_2$S$_4$ nanocomposites at low temperature.

UV-vis spectra for MB and Rh.B solution degraded by as-prepared composites sonophotocatalysts under visible light irradiation were recorded using a UV-Vis (Optizen Pop Mecasys Co., Ltd., Korea) spectrometer.

2.5 Photocatalytic studies

The photocatalytic activity of the sample such as P25, pure CdLa$_2$S$_4$, and GR-CdLa$_2$S$_4$ nanocomposite were evaluated by the degradation of MB and Rh.B solution under irradiation of visible light (8W, Fawoo, Lumidas-H, Korea, $\lambda > 420$ nm). In an ordinary photocatalytic test performed at room temperature, 0.05 g photocatalyst was added to 50 mL of 2.0×10^{-5} mol/L MB solution, which was hereafter considered as the initial concentration (c_0).

To achieve more degradation activity of the GR-CdLa$_2$S$_4$ nanocomposite industrial dye, Rh.B was also conducted at a high cconcentration (50 mL, 3.0×10^{-5} mol/L).

The mixture was sonicated for 10 min and stirred for 120 min in the dark in order to reach adsorption–desorption equilibrium. The first sample was taken out just before the light was turned on in order to determine the dye concentration in solution after dark adsorption, which was henceforth considered as the initial concentration (c_{ads}). Samples were then withdrawn regularly from the reactor by orders of 30 min, 60 min, 90 min, and 120 min and immediately centrifuged to separate any suspended solid. The clean transparent solution was analyzed by using a UV-Vis spectrophotometer at wavelengths from 250 nm to 800 nm.

3. Results and Discussion

3.1 Characterization

Figure 2(b) shows the XRD pattern of the product obtained from the above procedure. It can be seen that the diffractogram of graphene exhibits the typical peaks at 25.9° and 42.7°, corresponding to the graphite (002) and (100) reflections (Joint Committee for Powder Diffraction Studies (JCPDS) No. 01-0646),[20] respectively. In CdLa$_2$S$_4$ and GR-CdLa$_2$S$_4$ composite, all the diffraction peaks could be indexed to CdLa$_2$S$_4$, indicating that single-phase CdLa$_2$S$_4$ was obtained. No peaks of other phases, such as CdS and La$_2$S$_3$, were found. This result is consistent with previous reports.[17] All diffraction peaks of CdLa$_2$S$_4$ remained unchanged after rinsing with distilled water and ethanol for several times, indicating that the present CdLa$_2$S$_4$ photocatalyst is stable in aqueous solution. However, no signal for any other phases of GO (001) or graphene (002) can be detected in GR-CdLa$_2$S$_4$ composite. According to a Ref.,[21] GO can be reduced to graphene during the solvothermal reaction and the synthesized graphene sheets can restack to form poorly-ordered graphite along the stacking direction. Earlier studies have shown that if the regular stack of GO or graphite is broken, for example, by exfoliation, their diffraction peaks may also become weak or even disappear.[22]

The morphologies of CdLa$_2$S$_4$, graphene and GR-CdLa$_2$S$_4$ nanocomposites were investigated by SEM. As show in Fig. 3(a), pure CdLa$_2$S$_4$ particles appear as spherical particles with good dispersion and large size. From this figure, the overall structure can be clearly predicted such that graphene is a plate-like structure broken off in different
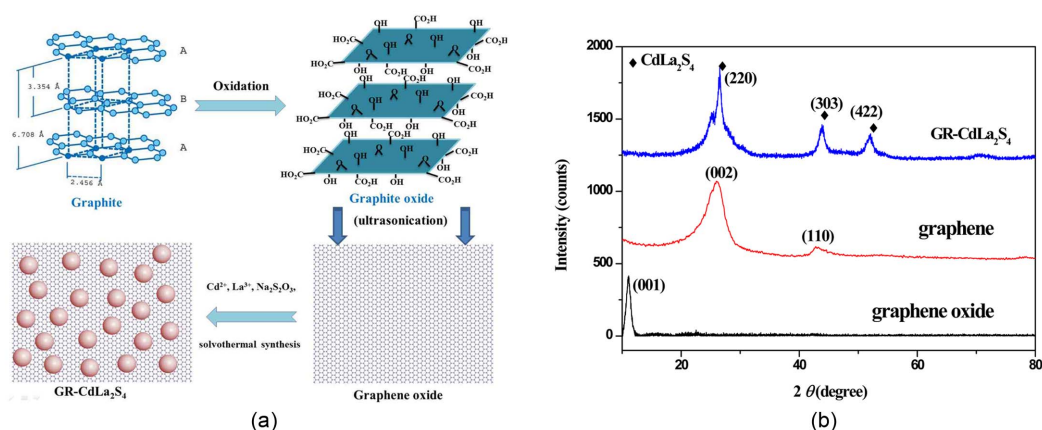

Fig. 2. (a) Schematic illustration of deposition of CdLa$_2$S$_4$ on the graphene, (b) XRD pattern of graphene oxide, graphene, and GR-CdLa$_2$S$_4$ composite.
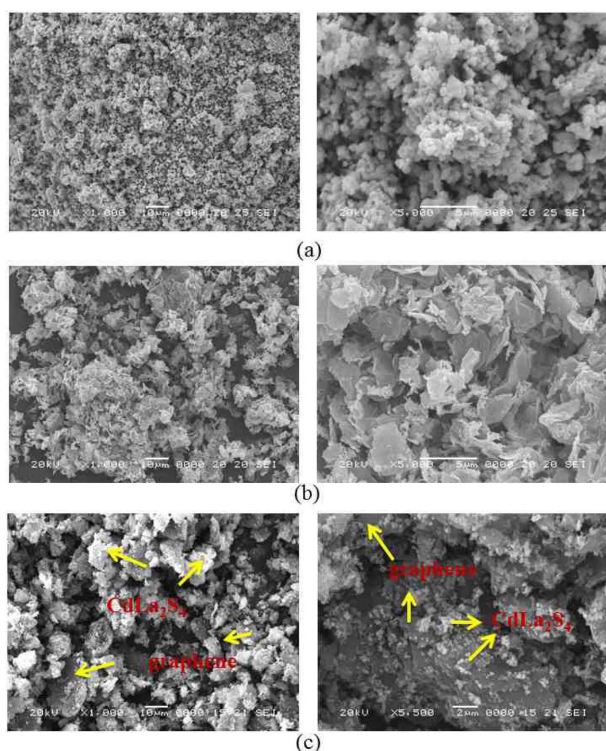
Fig. 3. SEM images of as-prepared samples: (a) pristine CdLa$_2$S$_4$, (b) graphene, and (c) GR-CdLa$_2$S$_4$ composites.

directions. A flake-like morphology was observed for graphene, reflecting its layered microstructure (Fig. 3(b)). The large interlayer spaces and thin layer edges of graphene can be clearly observed. The morphology of GR-CdLa$_2$S$_4$ composites has a substantial difference from that of the graphene sheets. Meanwhile, the spherical CdLa$_2$S$_4$ nanoparticles with smaller size compared with pure CdLa$_2$S$_4$ can be observed, which were tightly and evenly distributed on

graphene sheets and formed a graphene-based nanostructure composite. Because of the presence of oxygen functionalities on the surface of the graphene sheet, electrostatic force arises among them in the form of Van der Walls interaction, in which the graphene sheet tends to aggregate back to graphitic structure. The attachment of nanoparticles on a graphene sheet is helpful to overcome these interactions.[23] The graphene sheet acts like a support material to CdLa$_2$S$_4$ particles that may be advantageous to supply a path for the generated electron and, as a result, will improve the photocatalytic behavior of the nanocomposites.

To get information about the change in element weight %, the prepared GR-CdLa$_2$S$_4$ composite was examined by EDX. Fig. 4 shows the EDX microanalysis and element weight % of GR-CdLa$_2$S$_4$ composite, which show the existence of C, Cd, La, and S. The strong C signal probably originates mainly from graphene nanosheets. The Lα_1 and L$_{\beta 1}$ peaks from the La element appear at 4.65 and 5.04 KeV, respectively, while the S peak comes from the precursor materials; Na$_2$S$_2$O$_3$ appears at Kα_1 2.309 KeV. Table 2 lists the numerical results of the EDX quantitative microanalysis of the samples.

3.2 Adsorption process and photodecolorization

Two steps are involved in the photocatalytic decomposition of dyes: the adsorption of dye molecules and photodegradation. Since the photo-oxidation reaction usually takes place at the catalyst surface, the adsorption characteristics of the system are expected to be quite important on the photocatalytic process. The ability of the MB to be adsorbed on the nanocomposite surface was tested using suspensions of MB and control sample P25, pure CdLa$_2$S$_4$, and GR-CdLa$_2$S$_4$ composite in dark conditions. The dye adsorbs onto these samples, and after the first 2 h, a clear decrease in the MB solution concentration is shown in Fig. 5. After this period, the adsorption–desorption equilibrium is achieved, and no more
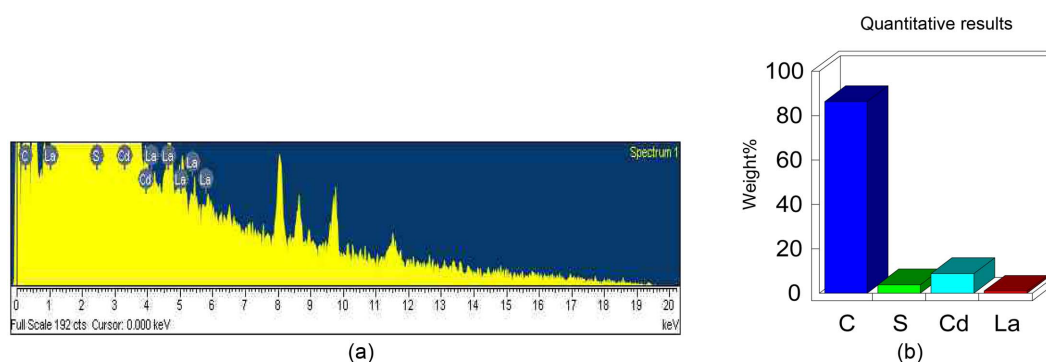

Fig. 4. EDX elemental microanalysis (a) and element weight % (b) of GR-CdLa$_2$S$_4$composite.

Table 2. EDX Elemental Microanalysis and BET Surface Areas of As-prepared Samples

Sample name	C (%)	O (%)	Ti (%)	Cd (%)	La (%)	S (%)	BET (m^2/g)
P25	_	45.22	54.78	_	_	_	18.95
CdLa$_2$S$_4$	_	_	_	4.84	9.47		31.73
GR-CdLa$_2$S$_4$	86.49	_	_	8.82	0.9	3.8	66.82
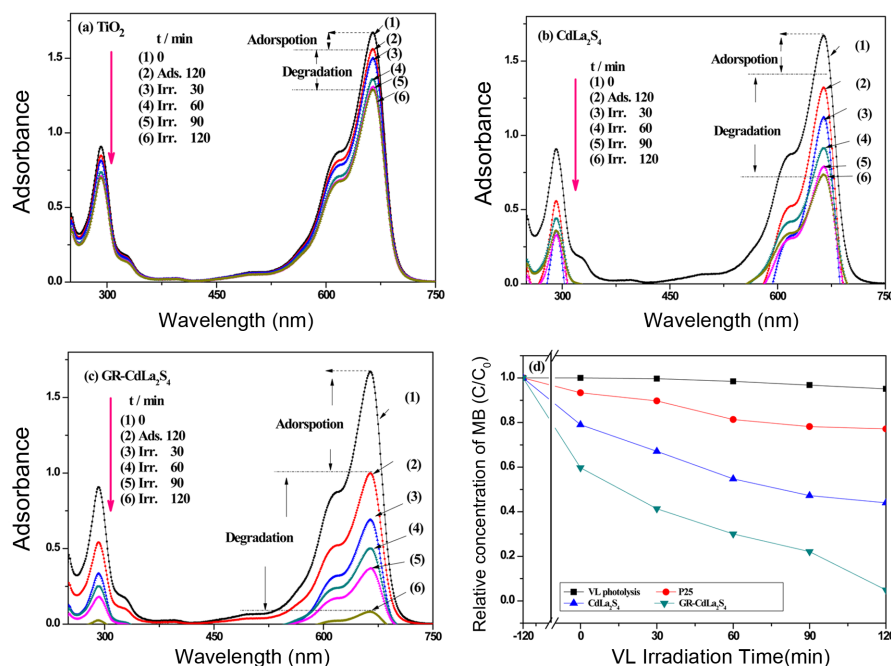
Fig. 5. UV-Vis absorption spectra for MB (2×10^{-5} mol/L, 50 mL) degradation by (a) P25, (b) CdLa$_2$S$_4$, and (c) GR-CdLa$_2$S$_4$, and (d) a plot of MB degradation efficiency visible light (VL) irradiation time.

decrease on the MB concentration occurs. The BET surface area of control sample P25, as well as as-prepared pure CdLa$_2$S$_4$ and GR-CdLa$_2$S$_4$ nanocomposites, were 18.95 m^2/g, 31.73 m^2/g, and 66.82 m^2/g, respectively. The effect of catalyst composition on MB (2.00×10^{-5} mol/L, 50 mL) degradation efficiency was investigated under visible light irradiation with a catalyst amount of 0.05 g. As shown in Fig. 5, the adsorption effect of GR-CdLa$_2$S$_4$ was better than that of any other sample due to the relatively higher surface area. The adsorptive effect of control sample TiO$_2$ was the lowest. GR-CdLa$_2$S$_4$ has the largest BET surface area, which can enhance the adsorptive effect.

Figure 5 also shows the change in the concentration of MB with different irradiation time in the presence of different photocatalysts, from which we can obviously see that the pure TiO$_2$ has little photocatalytic activity toward the photodegradation of MB solution. The MB solution degraded better, when introducing CdLa$_2$S$_4$ particles. In contrast, it indicates that the MB molecules could be excellently degraded in the presence of GR-CdLa$_2$S$_4$ composites. The degradation efficiency of MB with all samples generally under visible light follows the order of GR-CdLa$_2$S$_4$ > CdLa$_2$S$_4$ > P25, from which we can obviously see that the GR-CdLa$_2$S$_4$ composites have a more excellent photocatlytic activity toward the photodegradation of methylene blue, which is due to the following reasons: (1) graphene nanosheets with wondrously high charge mobility acting as good electron acceptors,[12-14] are expected to improve the interfacial electron transfer and restrain the electron/hole (e$^-$/h$^+$) pair recombination of GR-CdLa$_2$S$_4$ and (2) graphene nanosheets with extremely high specific surface area[23] can

enhance the dispersion of CdLa$_2$S$_4$ nanoparticles and allow for greater photon absorption on the photocatalytic surface.

To demonstrate the photocatalysis activity and cyclic performance of the GR-CdLa$_2$S$_4$ photocatalyst, consecutive photocatalytic, degradation reactions with higher Rh.B concentration were conducted in the presence of GR-CdLa$_2$S$_4$ under visible light irradiation. Moreover, the dye solution increasingly lost its color intensity as the dye concentration continued to decrease. The decrease in concentration was evaluated at the λ_{max} values of the dye, which were determined from the absorption spectra of the dyes. The λ_{max} value of Rh.B was found to be 554 nm. In the case of GR-CdLa$_2$S$_4$, Rh.B (3×10^{-5} mol/L, 50 mL) was photodegraded to of 55.6% after achieving adsorption–desorption equilibrium at the end of 120 min, shown in Fig. 6(a). As shown in Fig. 6 (b,) GR-CdLa$_2$S$_4$ exhibited no significant loss of photocatalytic activity after four runs of Rh.B degradation. These results indicate that the GR-CdLa$_2$S$_4$ photocatalyst has high stability and does not photocorrode during the photocatalytic oxidation of Rh.B. Thus, the GR-CdLa$_2$S$_4$ composite is promising for practical photocatalyst applications in environmental purification. Graphene modification improves not only the photocatalytic performance but also the long-term stability of CdLa$_2$S$_4$ nanocrystals. This result is significant from a practical viewpoint, as the enhanced photocatalytic activity and stability will lead to more cost-effective operation. These results further confirm that GR-CdLa$_2$S$_4$ nanocomposite can be used as catalytic material in environmental purification processes or in waste water treatment in the future.

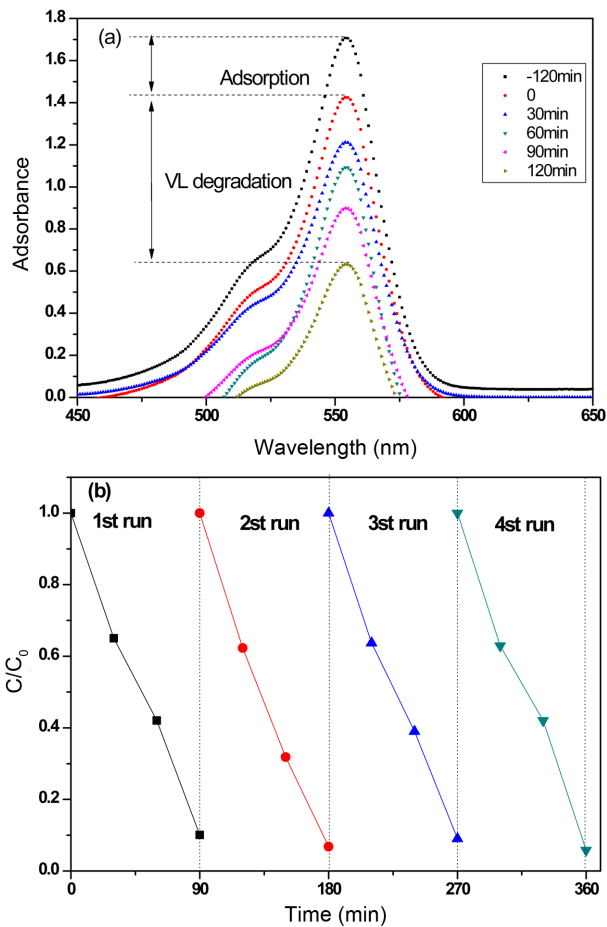The scheme of the charge transfer process between

Fig. 6. (a) UV-Vis spectra of Rh.B $(3 \times 10^{-5}$ mol/L, 50 mL) concentration and cycling runs (b) against GR-CdLa$_2$S$_4$composite under visible light.
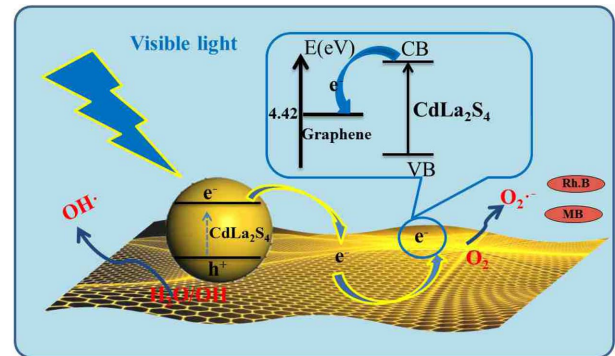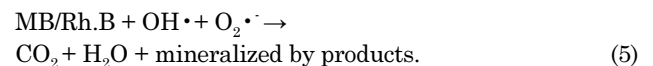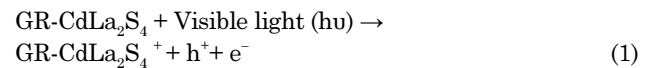

Fig. 7. The scheme of degradation MB, Rh.B dyes on the interface of CdLa$_2$S$_4$, and graphene nanosheet under visible light irradiation.

form hydroxyl radicals OH$\cdot$[24]. The MB and Rh.B molecules then can be photocataytically degraded by oxygen peroxide radicals O$_2$$\cdot^-$ and hydroxyl radicals OH$\cdot$ to CO$_2$, H$_2$O, and other mineralization products. The reactions involved in the charge mobility and mineralization of the dyes are as follows:

$$\text{GR-CdLa}_2\text{S}_4 + \text{Visible light (h}\upsilon) \rightarrow$$
$$\text{GR-CdLa}_2\text{S}_4{}^+ + \text{h}^+ + \text{e}^- \tag{1}$$

$$\text{H}_2\text{O} \rightarrow \text{H}^+ + \text{OH}^- \tag{2}$$

$$\text{h}^+ + \text{OH}^- \rightarrow \text{OH}\cdot \tag{3}$$

$$\text{O}_2 + \text{e}^- \rightarrow \text{O}_2\cdot^- \tag{4}$$

$$\text{MB/Rh.B} + \text{OH}\cdot + \text{O}_2\cdot^- \rightarrow$$
$$\text{CO}_2 + \text{H}_2\text{O} + \text{mineralized by products.} \tag{5}$$

4. Conclusions

In this study, GR-CdLa$_2$S$_4$ visible-light-responsive composite photocataysts were synthesized by a facile solvothermal method. The formed CdLa$_2$S$_4$ was triggered by a precipitation reaction uniformly distributed on the graphene sheets. SEM images show that CdLa$_2$S$_4$ nanoparticles were attached to a graphene sheet. From the EDX data, the main elements like Cd, La, S, C existed in the composites. The catalytic activity of GR-CdLa$_2$S$_4$ composites were examined by degradation of organic dyes in aqueous solutions under visible light irradiation. These results reveals the exceptional feature of graphene that makes it an excellent supporting material for semiconductor nanoparticles as an electron acceptor and transporter. Predominantly, this research results offer some significant evidence about the visible light active photocatalytic degradation process and its catalytic mechanism.

Acknowledgments

CdLa$_2$S$_4$ particles and graphene is shown in Fig. 7. When GR-CdLa$_2$S$_4$ was illuminated with visible light, the semiconductor (metal selenide) produced electrons (e$^-$) and holes (h$^+$) that gained enough energy or momentum to jump the forbidden gap or energy barrier denoted as (E$_g$). The electrons (e$^-$) traveled from the valence band (VB) to the conduction band (CB), producing an increased number of electrons (e$^-$) in the conduction band (CB) and holes (h$^+$) in the valence band (VB). Thus, a number of electrons (e$^-$) and holes (h$^+$) were generated in CdLa$_2$S$_4$. Meanwhile, graphene attached to the semiconductor material CdLa$_2$S$_4$ assisted in the smooth transistion transferring electrons (e$^-$) to the CB of CdLa$_2$S$_4$, thereby increasing the number of electrons as well as the rate of electron-induced redox reactions. Based on the above discussion, the graphene in GR-CdLa$_2$S$_4$ nanocomposite not only improved the visible light absorption intensity but also enhanced the photocatalytic activity of the nanocomposites because of the high charge seperation induced by the synergistic effects of graphene on CdLa$_2$S$_4$. The generated electrons (e$^-$) react with dissolved oxygen molecules and produce oxygen peroxide radicals O$_2$$\cdot^-$. The positive charge hole (h$^+$) can react with OH$^-$ derived from H$_2$O to

REFERENCES

1. K.S. Novoselov, A.K. Geim, S.V. Morozov, D. Jiang, Y. Zhang, S.V. Dubonos, I.V.Grigorieva, and A.A. Firsov, "Electric Feld Effect in Atomically Thin Carbon Flms," *Science*, **306** 666-69 (2004).

2. C. Lee, X. Wei, J.W. Kysar, and J. Hone, "Measurement of the Elastic Properties and Intrinsic Strength of Monolayer Graphene," *Science*, **321** 385-88 (2008).

3. B. Tang, G.X. Hu, and H.Y. Gao, "Raman Spectroscopic Characterization of Graphene," *Appl. Spectrosc. Rev.*, **45** 369-407 (2010).

4. S.M. Peak, E.J. Yoo, and I. Honma, "Enhanced Cyclic Performance and Lithium Storage Capacity of SnO_2/Graphene Nanoporous Electrodes with Three-dimensionally Delaminated Fexible Structure," *Nano Lett.*, **9** 72-75 (2009).

5. B. Seger and P.V. Kamat, "Electrocatalytically Active Graphene–platinum Nanocomposites. Role of 2-D Carbon Support in PEM Fuel Cells," *J. Phys. Chem.*, C **113** 7990-95 (2009).

6. M.R. Hoffmann, S.T. Martin, W. Choi, and D.W. Bahnemann, "Environmental Applications of Semiconductor Photocatalysis," *Chem. Rev.,* **95** 69-96 (1995).

7. N.S. Lewis, "Light Work with Water," *Nature,* **414** 589-90 (2001).

8. M.H. Huang, S. Mao, H. Feick, H.Q. Yan, Y.Y. Wu, H. Kind, E. Weber, R. Russo, and P.D. Yang, "Room-temperature Ultraviolet Nanowire Nanolasers," *Science,* **292** 1897-99 (2001).

9. M.A. Kolb, W.F. Maier, and K. Stöwe, "High-throughput Syntheses of Nano-scaled Mixed Metal Sulphides," *Catal. Today,* **159** 64-73 (2011).

10. G. C. Chinchen and M. S. Spencer, "A Comparison of the Water-Gas Shift Reation on Chromia-Promoted Magnetite and on Supported Copper Catalysts," *J. Catal.*, **112** 325-27 (1988).

11. B.L. Abrams and J.P.Wilcoxon, "Nanosized Semiconductors for Photooxidation," *Crit. Rev. Solid State Mater. Sci.,* **30** 153-82 (2005).

12. A.N. Cao, Z. Liu, S.S. Chu, M.H. Wu, Z.M. Ye, Z.W. Cai, Y.L. Chang, S.F. Wang, Q.H. Gong, and Y.F. Liu, "A Facile One-step Method to Produce Graphene–CdS Quantum Dot Nanocomposites as Promising Optoelectronic Materials," *Adv. Mater.*, **22** 103-06 (2010).

13. C. Nethravathi, T. Nisha, N. Ravishankar, C. Shivakumara, and M. Rajamathi, "Graphene-nanocrystalline Metal Sulphide Composites Produced by a One-pot Reaction Starting from Graphite Oxide," *Carbon*, **47** 2054-59 (2009).

14. H.T. Hu, X.B. Wang, F.M. Liu, J.C.Wang, and C.H. Xu, "Rapid Microwave-assisted Synthesis of Graphene Nanosheets–zinc Sulfide Nanocomposites: Optical and Photocatalytic Properties," *Synthetic. Metals.*, **161** 404-10 (2011).

15. B.B. Kale, J.O. Baeg, K.J. Kong, S.J. Moon, L.K. Nikam, and K.R. Patil, "Self Assembled $CdLa_2S_4$ Hexagon Flowers, Nanoprisms and Nanowires: Novel Photocatalysts for Solar Hydrogen Production," *J. Mater. Chem.*, **21** 2624-31 (2011).

16. Y.P. Yuan, S.W. Cao, L.S. Yin, L. Xu, and C.Xue, "NiS_2 Cocatalyst Decoration on $CdLa_2S_4$ Nanocrystals for Efficient Photocatalytic Hydrogen Generation Under Visible Light Irradiation," *Int. J. Hydrogen. Energy*, **38** 7218-23 (2013).

17. J.G. Hou, C. Yang, Z. Wang, S.Q. Jiao, and H.M. Zhu, "Hydrothermal Synthesis of $CdS/CdLa_2S_4$ Heterostructures for Efficient Visible-light-driven Photocatalytic Hydrogen Production," *RSC Adv.*, **2** 10330-06 (2012).

19. W.C. Oh and F.J. Zhang, "Preparation and Characterization of Graphene Oxide Reduced From a Mild Chemical Method," *Asian. J. Chem.*, **23** 875-79 (2011).

20. D. Li, M.B. Muller, S. Gilje, and G.G. Wallace, "Processable Aqueous Dispersions of Graphene Nanosheets," *Nat. Nanotechnol.*, **3** 101-05 (2008).

21. W.C. Oh, F.J. Zhang, and M.L. Chen, "Characterization and Photodegradation Characteristics of Organic Dye for Pt-titania Combined Multi-walled Carbon Nanotube Composite Catalysts," *J. Ind. Eng. Chem.*, **16** 321-26 (2010).

22. H. Zhang, X.J. Lv, Y.M. Li, Y. Wang, and J.H. Li, "P25-graphene Composite as a High Performance Photocatalyst," *ACS Nano.*, **4** 380-86 (2010).

23. D. Cai and M. Song, "Preparation of Fully Exfoliated Graphite Oxide Nanoplatelets in Organic Solvents," *J. Mater. Chem.*, **17** 3678-80 (2007).

24. S. D. Perera, R. G. Mariano, K. Vu, N. Nour, O. Seitz, Y. Chabal, and K. J. Balkus. Jr, "Hydrothermal Synthesis of Graphene-TiO_2 Nanotube Composites with Enhanced Photocatalytic Activity," *ACS Catal.*, **2** 949-56 (2012).